

Smoothing turbulence-induced power fluctuations in large wind farms by optimal control of the rotating kinetic energy of the turbines

This content has been downloaded from IOPscience. Please scroll down to see the full text.

2014 J. Phys.: Conf. Ser. 524 012187

(<http://iopscience.iop.org/1742-6596/524/1/012187>)

View [the table of contents for this issue](#), or go to the [journal homepage](#) for more

Download details:

IP Address: 134.58.253.57

This content was downloaded on 27/06/2014 at 08:46

Please note that [terms and conditions apply](#).

Smoothing turbulence-induced power fluctuations in large wind farms by optimal control of the rotating kinetic energy of the turbines

Johan Meyers

Department of Mechanical Engineering, KU Leuven, Celestijnenlaan 300A, B3001 Leuven, Belgium

E-mail: johan.meyers@kuleuven.be

Simon De Rijcke, Johan Driesen

Department of Electrical Engineering – ESAT, KU Leuven, Kasteelpark Arenberg 10, B3001 Leuven, Belgium

Abstract. In the current study, we use a large-eddy simulation of a wind-farm boundary layer to generate the fluctuating wind fields that are observed at different turbines in the wind farm. Using these wind fields as inputs, we focus on the development of a benchmark framework in which we explore the trade-off between high energy extraction and low variability using optimal control of multiple turbines subject to a turbulent wind field. The controls variables that are optimized are the electric torque and the pitch angles of the individual turbines over time horizons of 10 minutes. Moreover, both optimal control of individual turbines and coordinated optimal control of groups of turbines are investigated. Optimal control results are presented in terms of Pareto fronts that show optimal trade-offs between energy extraction and power smoothing. We find that power variations can be significantly reduced with limited loss of extracted energy. Moreover, coordinated control can effectively reduce fluctuations over longer time scales. For instance, considering 24 optimally coordinated turbines, variability at a time scale of 50 seconds is reduced 4 times more than the normal statistical reduction of 24 uncoordinated turbines.

1. Introduction

In large wind farms, turbulence that is induced by turbine wakes increases the overall wind-farm turbulence to levels that are considerably higher than that of the background atmospheric boundary layer [1]. Consequently, also the power variability increases significantly: this is mostly observed in a range of timescales from a few seconds to several minutes. However, since turbines have rotational masses, they all have a large rotating kinetic energy. This kinetic energy may be potentially exploited to smooth the electric power output, by temporarily increasing or decreasing the turbines' rotation, instead of directly feeding all of the fluctuating aerodynamic power to the generator. In the current work, we investigate the use of optimal coordinated control of wind turbines to smooth electric power, and explore optimal trade-offs between smoothing power and maximizing energy extraction. The nature of this trade-off is discussed in detail.



Wind-turbine operation is often classified into three regions: I–III [2]. The first region is at very low wind speeds where aerodynamic forces cannot overcome the turbine’s internal friction losses. At very high wind speeds (Region III), the power output of turbines is restricted by loading constraints on its mechanical structures and by economical constraints on the size of the power generator. In this region, turbine power is controlled at a constant level, independent of wind speed, and thus, power variability remains limited. In Region II, power output is not restricted, and wind turbines adapt their rotational speed and power output to the wind speed, yielding large variability in power output. Consequently, we focus in the current work on Region II operation.

In current-day regulation and market conditions, power variability of wind farms is not penalized as long as the provided energy blocks (with a duration of e.g. 10 or 15 min) fulfills the scheduled nomination. However, this situation may change in the future. This is related to the need for frequency regulation in the power system: at all times, the power generated in power plants should equal the power used by consumers. Any imbalance will slow down (or speed up) the rotating machines delivering the power, thus changing the system frequency. The inertia of the system is essentially related to the total mechanical inertia of all rotating synchronous generators coupled to the grid. This inertia introduces a time delay that gives governors time to react to frequency variations and assist in the task of frequency regulation. With more synchronous generators replaced by wind power plants, more power variability is added to the system, and relatively less operating reserves for frequency regulation (less governing action) are available. If the contribution of wind energy in the overall electricity production mix keeps increasing, this may lead to changes in grid regulations (e.g. penalizing variability), and market conditions (e.g. a market for ancillary services) to relieve the burden of frequency regulation and make power smoothing in wind farms economically interesting.

In the current study, it is not our aim to perform an in-depth analysis of such potential economic scenarios. Instead, we investigate the technical potential of power smoothing. To that end, we concentrate on power smoothing in large wind farms with fluctuating velocity fields that are obtained from time-resolved turbulent-flow simulations, i.e. based on large-eddy simulations [3, 4]. This provides realistic turbulent wind data with representative temporal and spatial coherence. We further focus on optimal control of rotating kinetic energy in the wind farm. This is achieved by optimally controlling the generator torque (allowing the turbine to speed up or slow down), combined with optimal pitching of the blades. Although such optimal control is difficult to implement in reality, it provides a benchmark for optimal trade-offs between power smoothing and energy extraction in wind farms.

In principle, changes in angular velocity of the turbines, and control of turbine pitch angles directly impact on the turbulent flow as a result of changing angles of attack, and lift and drag coefficients of the blade. However, if the turbulent flow is fully coupled into the optimal control problem, the system becomes very complex and expensive to solve (see Ref. [5]), prohibiting an extensive study of trade-offs between energy extraction and power smoothing. Therefore, we simplify the optimal control problem by presuming that the turbulent flow field (obtained from the LES) is insensitive to our control actions. Such a one-way coupled approach is justified provided that variations in the turbine thrust coefficient remain small. This is indeed the case for the relevant control cases as discussed in more detail in the manuscript.

Finally, optimal control results are presented in terms of Pareto fronts that show optimal trade-offs between energy extraction and power smoothing. We find that power variations can be significantly reduced with limited loss of extracted energy. If we limit power losses to a few percentages and look at a one-turbine case, we find that this mainly leads to smoothing of variations that have timescales below 10 seconds. In case of coordinated control (i.e. we included up to 24 turbines), variability with longer characteristic timescales can be reduced. For instance, restricting the energy-loss incurred by smoothing to 1%, and looking at timescales of

50 seconds, the variability of a coordinated case with 24 turbines is reduced with a factor of 6, compared to a factor of 1.4 for an uncoordinated case. We further study in detail how the regulating power that can be used for power smoothing depends on coordination of turbines in the wind farm.

2. Methodology

2.1. problem formulation

Consider a wind farm with N_t turbines, with rotational speeds ω_i ($i = 1 \cdots N_t$). Each of these turbines is subject to an aerodynamic torque $T_{a,i}$, and a generator torque $T_{e,i}$. Given these two torques, the Newton's second law for rotation for turbine i corresponds to

$$I \frac{d\omega_i}{dt} = T_{a,i}(V_{d,i}, \omega_i, \beta_i) - T_{e,i}, \quad (1)$$

where I the total moment of inertia. The aerodynamic torque depends on the wind speed $V_{d,i}$ at the turbine disk (for turbine i), which we obtain from large-eddy simulations. It further depends on the rotational speed ω_i , and the pitch angle β_i . To change the rotational speed of the turbine, and potentially store or deplete rotating kinetic energy, both the generator torque $T_{e,i}$, and the blade pitch β_i can be used as control inputs.

The wind speeds required in (1) are obtained from large-eddy simulations of a large wind-farm (cf. Ref. [3, 4]). Given the axial velocity $V_{d,i}(t)$ at turbine-disk level ($i = 1 \cdots N_t$), we use an empirical correlation to express the aerodynamic turbine torque as function of disk velocity, blade pitch angle, and angular velocity. We start from

$$P_i \equiv \frac{1}{2} C'_{p,i} \rho V_{d,i}^3 A = T_{a,i} \omega_i \quad \Rightarrow \quad T_{a,i} = \frac{C'_{p,i} \rho V_{d,i}^3 A}{2 \omega_i}, \quad (2)$$

with $A = \pi D^2/4$ the rotor area. Note that it is uncommon to use the disk velocity; usually the undisturbed free-stream velocity is used. However, in a large wind-farm, this is not unequivocally defined. Moreover, $V_{d,i}$ is readily available from the simulations. To express the disk-based power coefficient $C'_{p,i}$, we use a correlation for $C_{p,i}$ from Ref. [6, 7], i. e.

$$C_{p,i}(\lambda_i, \beta_i) = c_1(c_2 \gamma_i + c_3 \beta_i + c_4) e^{c_5 \gamma_i},$$

$$\text{with } \gamma_i = \frac{1}{\lambda_i + c_6 \beta_i} + \frac{c_7}{\beta_i^3 + 1}, \quad (3)$$

where $\lambda_i = R\omega_i/V_{i,\infty}$ is the tip-speed ratio. Further, $c_1 = 2.20 \times 10^{-1}$, $c_2 = 1.16 \times 10^2$, $c_3 = -4.00 \times 10^{-1}$, $c_4 = -5.00$, $c_5 = -1.25 \times 10^1$, $c_6 = 8.00 \times 10^{-2}$ and $c_7 = -3.50 \times 10^{-2}$. Finally, based on the LES set-up, and neglecting the effect of power-smoothing control actions on the flow field, we estimate $V_{i,\infty} \approx 4V_{d,i}/3$ (See Ref. [8] for details).

Given the model for the turbine rotational speeds in a wind farm, a optimal control framework is now defined in which the generator torques $\mathbf{T}_e(t) = [T_{e,1}(t), T_{e,2}(t), \cdots, T_{e,N_t}(t)]$, pitch angles $\boldsymbol{\beta}(t)$, and rotational speeds $\boldsymbol{\omega}(t)$ are optimized over a time horizon T . We consider a multi-objective optimization framework in which we investigate optimal trade-offs between energy extraction and power smoothing. This requires the definition of two related cost functionals. The first relates to the accumulated energy extraction over the time horizon T , i.e.

$$\mathcal{J}_1(\boldsymbol{\omega}, \mathbf{T}_e, T) = - \int_0^T P_f(\boldsymbol{\omega}, \mathbf{T}_e) dt = \int_0^T - \sum_{i=1}^N T_{e,i}(t) \omega_i(t) dt, \quad (4)$$

with P_f the power extracted by the wind farm, and where a minus sign is introduced in the cost functional as it will be used in a minimization problem. The second cost functional relates to the smoothing of power gradients, i.e. [8]

$$\mathcal{J}_2(\boldsymbol{\omega}, \mathbf{T}_e, \boldsymbol{\beta}, T) = \int_0^T \left(\int_t^{t+\tau} \frac{dP_f}{dt'} dt' \right)^2 dt \quad (5)$$

$$= \int_0^T \left(P_f(\boldsymbol{\omega}(t), \mathbf{T}_e(t)) - P_f(\boldsymbol{\omega}(t-\tau), \mathbf{T}_e(t-\tau)) \right)^2 dt. \quad (6)$$

In this second cost functional, we define power gradients averaged over a time τ , for which we select $\tau = 1\text{sec}$ (cf. also Ref. [8] for a more detailed discussion).

Given the cost functionals \mathcal{J}_1 and \mathcal{J}_2 , the multi-objective optimal control problem is now defined as

$$\min_{\boldsymbol{\omega}, \mathbf{T}_e} \quad \alpha \mathcal{J}_1 + (1 - \alpha) \mathcal{J}_2, \quad (7)$$

$$\text{subject to} \quad I \frac{d\boldsymbol{\omega}}{dt} - \mathbf{T}_a(\mathbf{V}_\infty, \boldsymbol{\omega}, \boldsymbol{\beta}) + \mathbf{T}_e = 0, \quad (8)$$

where we vary $\alpha \in [0, 1]$ in order to construct a Pareto front, which is a curve that shows optimal trade-offs between two optimization objectives (in case of more dimensions, it becomes a (hyper) surface). In the current work Pareto fronts are used to explore different optimal trade-offs between \mathcal{J}_1 and \mathcal{J}_2 .

2.2. Computational set-up

To solve the optimization problem, the system is first discretized in time. To that end, the state variables $\boldsymbol{\omega}(t)$ are sampled every 0.2 sec, and Eq. (8) is discretized using the trapezoid rule according to Newton–Cotes. The controls $\boldsymbol{\beta}(t)$ and $\mathbf{T}_e(t)$ are allowed to change every 1.0 sec and remain constant during the intermediate time steps of the states. Given the frequency content of the wind signal ($< 0.5\text{Hz}$), and size of the inertia of the turbines, this discretization gives sufficient accuracy, i.e. further time-step refinement does not lead to noticeable differences in results. Finally, we remark that we do not include any constraints on the pitch rate, implicitly presuming no pitch inertia. However, in the optimal control results, the actual pitch rates remain well below $5^\circ/\text{s}$.

The optimization problem stated in Eqs. (7-8) is solved by a gradient based solver from TOMLAB/KNITRO [9]. This solver offers an iterative Conjugate Gradient (CG) approach for large scale problems, that is combined with a Sequential Linear-Quadratic Programming (SLQP) optimizer for fast convergence of results close to the optimum. The gradient of the cost-function is obtained by automatic differentiation that provides an automatic formulation of the discrete adjoint system, and is facilitated by the matrix formulation of the problem in the TOMLAB environment.

For the optimization time window, we select $T = 800\text{ sec}$. However, as a result of the nature of the optimization problem, all turbines decelerate to standstill at the end of the optimization time horizon. In fact, since the optimization is not considered beyond $t = T$, any remaining rotational energy in the turbines is considered useless by the algorithm, and instead it is fully depleted in favor of a larger total energy yield. This only occurs at the very end of the time horizon, i.e. towards $t = 800\text{ sec}$, and therefore we evaluate optimized results only up to $t = 650\text{ sec}$, discarding the last 150 seconds of the optimization time window. In addition, non-optimal initial conditions result in transients that decay very fast in time at the beginning of each simulation run. Thus, we also discard the first 50 seconds of the optimization window for postprocessing.

3. Results

In the previous section, we introduced the methodology for optimal power smoothing evaluated over a time window of 600 seconds, and subject to a turbulent velocity field obtained from large-eddy simulations. However, turbulence in a wind-turbine boundary layer is characterized by large variability, and timescales up to several hundreds of seconds. Thus one single time series of 600 seconds is in itself not sufficient to provide a statistically converged expectation of the gains of optimal power smoothing. To that end, the optimization results need to be averaged over a large set of different statistically independent turbulent time series. Therefore, we construct averaged Pareto fronts (scanning different values of $\alpha \in [0, 1]$) by using the averages of following derived properties [8]

$$\bar{E}_* = \frac{\frac{1}{n} \sum_{j=1}^n \mathcal{J}_{1,j}}{\left[\frac{1}{n} \sum_{j=1}^n \mathcal{J}_{1,j} \right]^{\alpha=1}}, \quad \text{and} \quad (9)$$

$$\bar{R}_* = \frac{\frac{1}{n} \sum_{j=1}^n \mathcal{J}_{2,j}}{\left[\frac{1}{n} \sum_{j=1}^n \mathcal{J}_{2,j} \right]^{\alpha=1}}, \quad (10)$$

respectively corresponding to the average energy extraction and average squared variability over n statistically independent optimization problems using different wind speed series of $T = 600$ sec that are extracted from the LES data for which in total 30000 seconds are available for 48 turbines. For further discussion, \bar{E}_* and $(\bar{R}_*)^{1/2}$ are used to evaluate the trade-off between energy extraction and power smoothing. In practice, we include approximately $n = 100$ independent optimization problems in the averages.

First of all, we look at the Pareto front for optimal control of a single turbine in Figure 1a. When decreasing α , gradually penalizing variability in the multi-objective optimization problem (cf. Eq. 7), we observe initially that variability $(\bar{R}_*)^{1/2}$ decreases considerably at almost no loss of total energy yield. Only when $(\bar{R}_*)^{1/2}$ is reduced below 0.4 [p.u] the energy yield starts to drop significantly. In Figure 1b, we show the power extracted as function of time, and for different values of $\alpha = 0.0, 0.1, 0.9, 1.0$ (also marked in Figure 1a). It is apparent that the electrical power signal is smoothed in time by lowering the weight α . When lowering α from 1.0 to 0.9, first power variations with high frequencies and smaller amplitudes are smoothed, at higher values of α , more power is smoothed, but also more energy is lost.

We now look into the benefit of coordinating turbines by looking at optimal coordinated control of up to 24 turbines. In Figure 2, the Pareto fronts are compared for 1, 2, 6, and 24 turbines, averaged over different time series from the LES data set. We keep using the normalization from Eqs. (9), and (10), so that $[(\bar{E}_*, \bar{R}_*)^{\alpha=1}] \equiv (1, 1)$. This allows for a direct comparison between the different cases. For instance, the one-turbine case in Figure 2 can be directly compared to the 24 turbine case, i.e., it is easily shown that the average over 24 uncoordinated optimally controlled turbines converges to the same Pareto front as that of the averaged one-turbine case. Similar arguments hold for the two- and six-turbine cases in Figure 2.

When comparing the different cases in Figure 2a, we observe a large benefit for coordinated power smoothing. The higher the number of turbines, the more variability can be reduced without losing significant amounts of extracted energy. We further compare two cases, A and B, where Case A corresponds to the coordinated optimal control of 24 turbines, and Case B the same 24 turbines that are individually controlled. Both cases are selected thus on the respective Pareto frontiers that their energy loss is 1% compared to optimal control of energy extraction at $\alpha = 1$. This is also marked on Figure 2a.

In Figure 2b the farm-power is shown for one time series in Case A, and Case B, showing that the former leads to a smoother signal in time. This is further corroborated in Figure 2c,

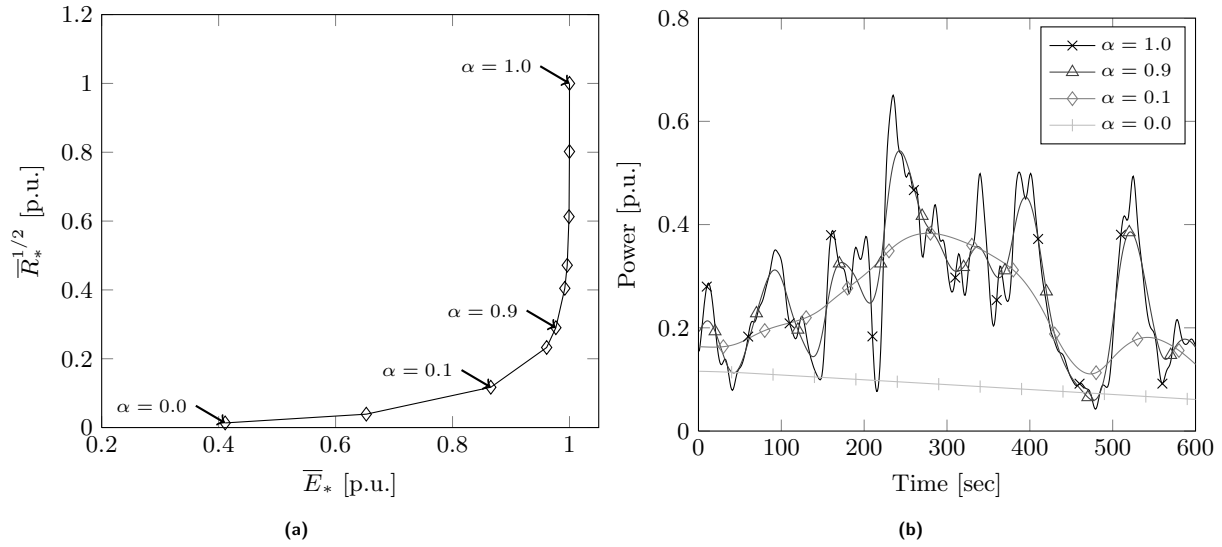


Figure 1. (a) Average Pareto front for a single turbine. This front shows the optimal trade-off between a reduction of power variations and maximization of energy extraction, by varying the weight $\alpha \in [0, 1]$. (b) Electrical power output for different points on the Pareto front for a representative time series of 600 sec.

where the power spectral density is shown for both cases. Here it is observed that mainly at lower frequencies (large timescales) coordinated control of multiple turbines outperforms single-turbine optimal control. For instance looking at frequencies around 20 mHz (a timescale of 50sec), variability is reduced with a factor of 6 for Case A with 24 turbines, compared to a factor of 1.4 only for an Case B.

Finally, we further explore cases A and B with respect to the regulating power that is used. To that end, for a turbine i , we define $P_{K,i} = dE_i/dt$, where $E_i = I\omega_i^2/2$ is the turbine's rotating kinetic energy. The total regulation of kinetic energy on farm level then corresponds to

$$P_{K,f} = \sum_{i=1}^{N_t} P_{K,i}. \quad (11)$$

This can be further split into the accelerating and decelerating actions, using

$$P_{K,f}^+ = P_{K,f}/2 + \sum_{i=1}^{N_t} |P_{K,i}|/2, \quad (12)$$

$$P_{K,f}^- = -P_{K,f}/2 + \sum_{i=1}^{N_t} |P_{K,i}|/2, \quad (13)$$

where by construction $P_{K,f} = P_{K,f}^+ - P_{K,f}^-$. Thus $P_{K,f}^+$ identifies how much power is being stored in accelerating turbines at a given time instance, while $P_{K,f}^-$ identifies how much power is being extracted at that time instance (remark that in a large farm, a number of turbines can be speeding up, while others are slowing down at the same time)

In Figure 3 $P_{K,f}$, $P_{K,f}^+$, and $P_{K,f}^-$ are shown for Case A (coordinated control), and Case B (uncoordinated control). First of all, it is interesting to observe in Figure 3a that $P_{K,f}$ has

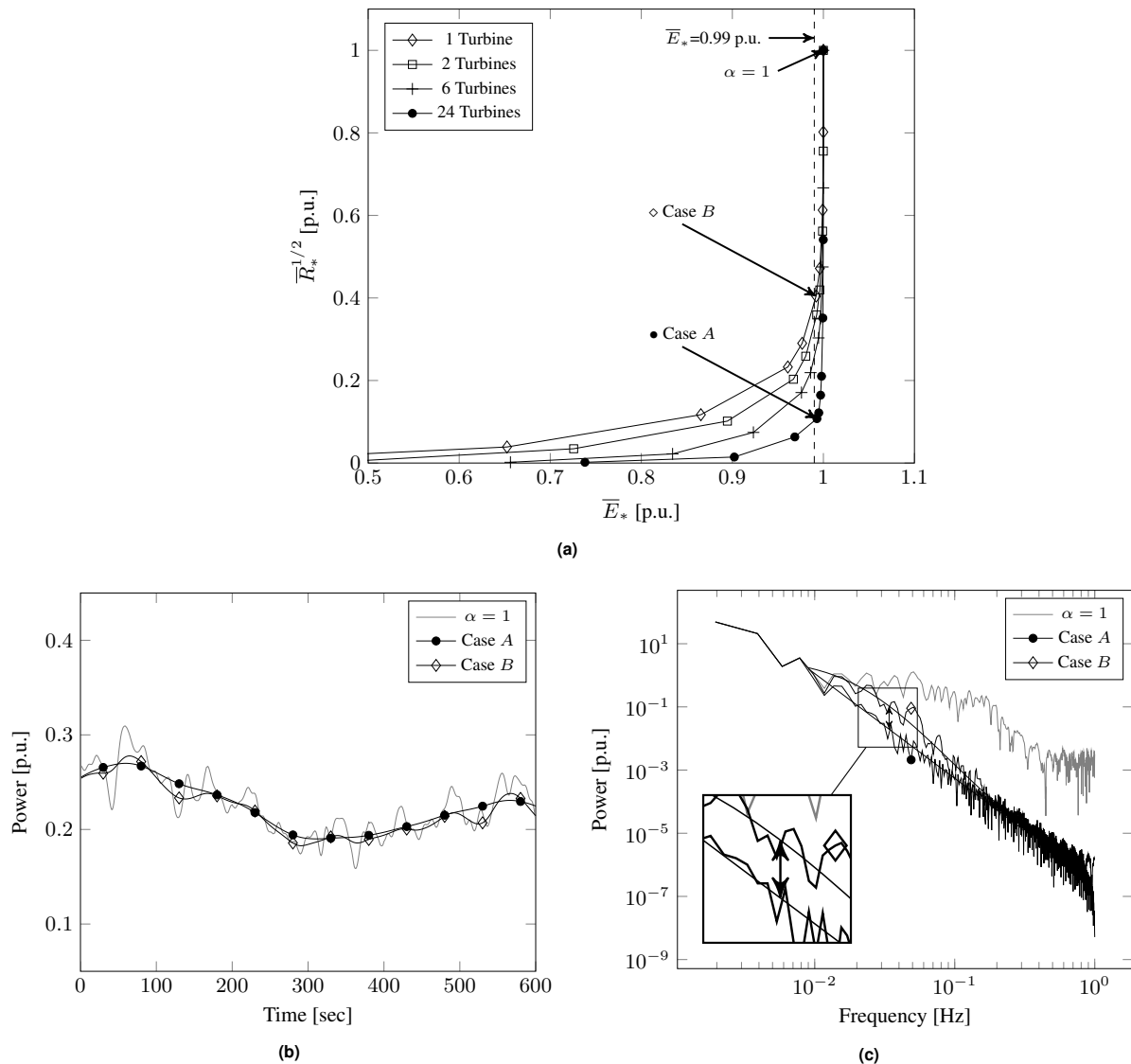


Figure 2. (a) Average Pareto front for respectively 1, 2, 6 and 24 turbines in a wind farm. The power elapse (b) and frequency spectrum (c) are illustrated for one time series handled in two cases: Case A with 24 turbines in the same optimization and Case B with the total power of separate optimization runs for the same 24 turbines. In (b), and (c) results are shown for points on the Pareto frontier for which the energy loss equals 1% compared to control without smoothing ($\bar{E}_* = 0.99$ p.u.), i.e. case A and B (also indicated on (a)).

roughly the same amplitude for both cases, but some of the peaks are higher for the coordinated case (Case A). Also when looking at Figure 3b, and c, it becomes apparent that peaks in $P_{K,f}^+$, and $P_{K,f}^-$ are higher for Case A than for Case B. This is a direct consequence of coordination. For an uncoordinated case, part of the turbines will accelerate, while others decelerate without taking into account the overall farm power output. For the coordinated case, more turbines will accelerate/decelerate simultaneously if required by a global dip in aerodynamic power; thus, leading to higher peaks for $P_{K,f}$, $P_{K,f}^+$, and $P_{K,f}^-$ when needed.

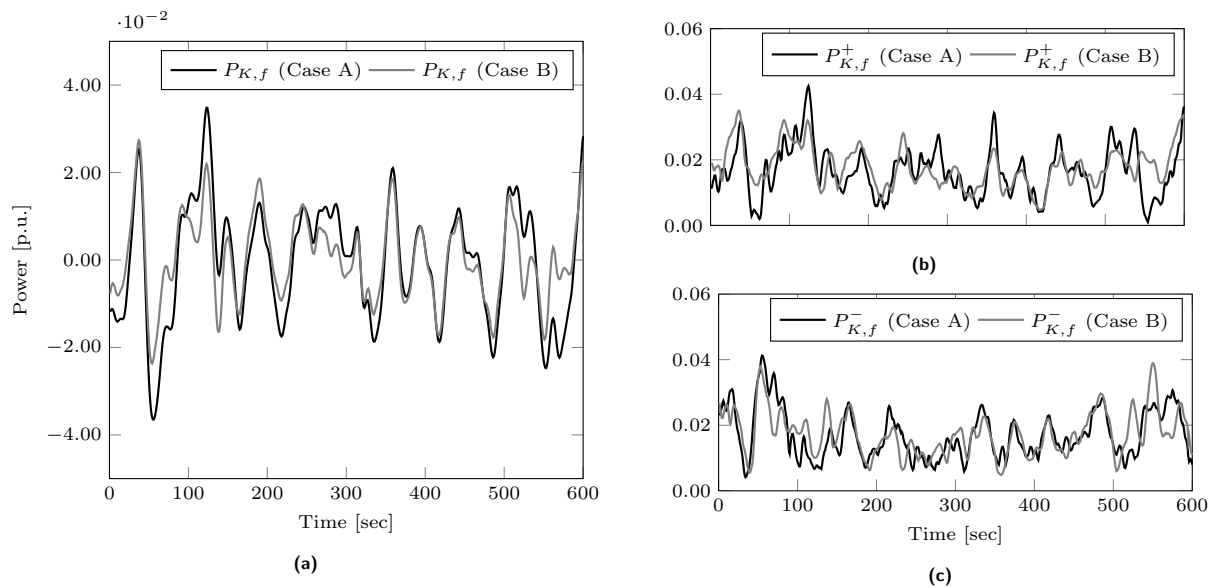


Figure 3. (a) regulating power $P_{K,f}$ for Case A (coordinated control) and Case B (uncoordinated control) (cf. also Figure 2); (a), and (b) accelerating power $P_{K,f}^+$ and decelerating power $P_{K,f}^-$ respectively for both cases.

4. Conclusions

We investigated optimal control of rotating kinetic energy in large wind farms, with the aim to smooth power variability originating from turbulent fluctuations of wind speeds. Pareto fronts were constructed, showing the optimal trade-off between reducing power variability, and maximizing energy extraction in the wind farm. We compared cases with uncoordinated optimal control with coordinated cases (up to 24 turbines), and showed that the latter are more effective at smoothing power without considerable losses of energy extraction. Moreover, coordinated cases also allow to smooth power variations with longer timescales, e.g., the case with 24 turbines was effective up to timescales of 1 minute.

Acknowledgments

The authors acknowledge financial support from the Research Foundation – Flanders (FWO, grant no. G.0376.12). J.M. further acknowledges support from the European Research Council (FP7-Ideas, grant no. 306471). Simulations were partly performed on the computing infrastructure of the VSC Flemish Supercomputer. The authors further thank TOMLAB for support on their optimization software.

References

- [1] Lebron J, Castillo L and Meneveau C 2012 *Journal of Turbulence* **13**
- [2] Burton T 2001 *Wind Energy Handbook* (Wiley & Sons)
- [3] Calaf M, Meneveau C and Meyers J 2010 *Physics of fluids* **22** 015110
- [4] Meyers J and Meneveau C 2013 *Journal of Fluid Mechanics* **715** 335–358
- [5] Goit J and Meyers J 2014 Optimal control of wind farm power extraction in large eddy simulations *AIAA SciTech 32nd ASME Wind Energy Symposium AIAA 2014-0709* (National Harbor, Maryland)
- [6] Slootweg J G, Polinder H and Kling W L 2001 Dynamic modelling of a wind turbine with doubly-fed induction generator *Vancouver IEEE Power Engineering Society Summer Meeting*
- [7] Heier S 2005 *Grid integration of wind energy conversion systems* (Wiley)

- [8] De Rijcke S, Driesen J and Meyers J 2014 *Wind Energy* **Submitted**
- [9] Rutquist P and Edvall M 2008 *User's Manual for TOMLAB* (1260 SE Bishop Blvd Ste E, Pullman, WA 99163, USA: Tomlab Optimization Inc.)